



Design of an integrated firefighting suit with hazardous gas monitoring and early warning applying a time series model

Yiwei Peng^b, Wenguo Weng^b, Xinyan Huang^a, Zhichao He^{a,b,*} 

^a Department of Building Environment and Energy Engineering, The Hong Kong Polytechnic University, Hong Kong Special Administrative Region of China

^b School of Safety Science (SSAFS), Tsinghua University, Beijing, China

ARTICLE INFO

Keywords:
Firefighting suit
Toxic gases
Time series prediction
Active protection
Hazard classification

ABSTRACT

Fire accident environments expose firefighters to life-threatening hazardous gases such as CO, HCN, and HCl, which can cause asphyxiation, organ damage, or even fatalities. Despite advancements in protective gear, conventional firefighting suits primarily offer passive protection, lacking real-time hazard forecasting. This reactive paradigm often results in delayed warnings against dynamic gas threats. This study proposes an innovative hardware-software integrated firefighting suit designed for proactive safety. The system combines wearable multi-gas sensors, edge computing, and a time series prediction model to forecast gas concentrations with 96.25 % accuracy. By analyzing historical data trends, the suit dynamically classifies hazard levels using a human vulnerability probit model, enabling proactive risk mitigation. Experimental results from simulated fire scenarios demonstrate superior performance in predicting concentrations of gases like H₂S and CO. The integration of predictive algorithms with real-time monitoring shifts safety management from passive response to proactive decision-making, enhancing firefighter survivability and operational efficiency. This advancement lays the foundation for next-generation intelligent firefighting equipment. This study is expected to provide a basis for the design of a kind of active protective firefighting suit.

1. Introduction

In firefighting scenarios, firefighting suits, as the core personal protective equipment for firefighters, directly affect the life safety of firefighters and the sustainability of firefighting operations. However, incidents of casualties caused by substandard firefighting suits remain frequent worldwide. Firefighting suits with inadequate thermal insulation properties in high-temperature environments may lead to heat stroke or severe burns, as exemplified by the case of an Arizona firefighter in the United States who succumbed to heat exhaustion while combating wildfires due to non-compliant protective clothing (U.S. Occupational Safety and Health Administration, 2013). Structural defects, such as insufficient seam strength, can also result in garment rupture, exposing firefighters to hazardous conditions—a situation illustrated by 5 Australian firefighter who suffered chemical burns during an industrial plant rescue when his protective suit tore (China National Emergency Broadcasting, 2019).

To address these issues, countries and regions have established

regulations like NFPA 1971 (U.S.) (National Fire Protection Association, 2018), EN 469 (EU) (European Committee for Standardization, 2020), and GA 10–2014 (China) (Ministry of Public Security of China, 2014), setting standards for flame resistance, thermal insulation, and chemical protection in firefighting suits. However, current standards still lack timeliness, enforcement, and systematic health monitoring for firefighters.

Fire environments produce toxic gases like CO, HCN, and H₂S, which can cause asphyxiation or organ damage, as well as corrosive HCl and HF. Flammable gases like methane can explode, worsening injuries. Exposure to these gases often leads to firefighter casualties. For example, the 2015 Tianjin Port explosion killed 110 firefighters due to explosions and toxic gases (China Chemical Safety Association, 2016), while the 2013 Santa Maria nightclub fire caused severe HCN poisoning in 10 firefighters (Couto et al., 2023). These incidents underscore the need for better protection, combining suit performance with gas detection and tactical alerts to reduce harm.

The passive protection of firefighting suits refers to the inherent

This article is part of a special issue entitled: APSS2025 published in Journal of Loss Prevention in the Process Industries.

* Corresponding author. Department of Building Environment and Energy Engineering, The Hong Kong Polytechnic University, Hong Kong Special Administrative Region of China.

E-mail address: zhichao.he@polyu.edu.hk (Z. He).

protective capability provided by the material's own flame-retardant, heat-insulating, and high-temperature-resistant properties (e.g., aramid, carbon fiber, etc.), which can defend against flames, thermal radiation, and high-temperature hazards (Chen et al., 2024). Its core characteristic lies in relying on the physicochemical attributes of the garment to achieve fundamental protection, thereby buying firefighters critical survival time. For instance, recent research has explored advanced materials such as nano-coated aramid to enhance fireproofing and thermal protection (Dong et al., 2025). Additionally, innovations in passive protection design, such as high-sweat-wicking thermal insulation suits, further improve comfort and safety by optimizing heat dissipation and moisture management (Xu et al., 2023).

Compared with passive protection, active protection in firefighting scenarios shows significant advantages in efficiency, early warning, and auxiliary decision-making, and has become a research hotspot in recent years (Blecha et al., 2018). Active protection can identify potential dangerous areas in advance and guide firefighters to avoid risks by real-time monitoring of fire environment parameters (e.g., temperature, gas concentration, flame spread rate) (Spitzenberger et al., 2016). This allows firefighters to focus more efficiently on key tasks, significantly improving the overall progress of firefighting operations. At the early warning level, active protection systems can predict fire development trends, toxic gas leaks, and deflagration risks through sensor networks and intelligent algorithms, issuing accurate alarms before dangers occur to buy valuable response time for firefighters (Mandal et al., 2018). In auxiliary decision-making, active protection integrates multi-dimensional fire data to generate visual situation analysis reports, providing a scientific basis for commanders to formulate more reasonable tactical strategies (e.g., optimizing rescue routes, allocating protective resources) (Shakeriaski et al., 2022). Thus, active protection fundamentally changes the passive response mode and builds a more proactive and intelligent safety protection system. Scholars have conducted research on firefighting suits in areas such as evacuation decision support (Zhang and Huang, 2024; Cheng et al., 2023), work duration estimation (Blecha et al., 2018), comfort design (Mandal et al., 2018; Zhang et al., 2023; Hur et al., 2013), and psychological cognition (Xu et al., 2025). However, little research on firefighting suits has focused on hazardous gases in firefighting environments, leaving a gap in the active protection design of firefighting suits.

To bridge this gap, this paper proposes a design of a hardware-software integrated firefighting suit that incorporates a time series prediction algorithm for monitoring typical hazardous gas concentrations in fire scenarios. The algorithm optimizes the parameters of an ARIMA (Autoregressive Integrated Moving Average)-based time series prediction model based on collected gas concentration data and generates predicted data for future periods. This study integrates protective equipment with dynamic hazardous gases monitoring and early warning. Based on the predicted data of hazardous gases, the integrated firefighting suit system can provide classified warnings on the risks of firefighting operations in the future period based on the human vulnerability model.

The innovation of this research is its focus on the hazardous gas environments faced by firefighters. The hardware-software integrated firefighting suit system can provide active and comprehensive protection, from hazardous gas concentration sensing to data processing, time series prediction, and hazard classification warning. The application of this research is expected to effectively reduce firefighter casualties in hazardous gas environments at fire scenes and improve firefighting efficiency. During the case study in fire brigade, this firefighting suit design has been well-received by firefighters.

This paper consists of four sections: Section 2 details the methodology, employing an ARIMA-based framework for gas concentration prediction and risk assessment. Section 3 validates the firefighting suit system design through simulated fire experiments in an actual firefighting scenario, demonstrating high prediction accuracy and the hazard classification process for hazardous gases. Section 4 summarizes

the study's contributions, highlighting the potential of time-series models in fire warnings and proposing future research directions for intelligent firefighting equipment. Section 5 provides some concluding remarks.

2. Methodology

This study presents a comprehensive system design for an active-protection firefighting suit, which integrates real-time gas monitoring, data processing, and predictive analytics to enhance firefighter safety. This section introduces the hardware-software integrated design of the firefighting suit, and focuses on the introduction of the hazardous gas monitoring and prediction algorithm based on a time series model.

2.1. Integrated design of firefighting suit system

As shown in Fig. 1, the firefighting suit system operates through three interconnected modules: (1) a sensor network that continuously collects and transmits toxic gas concentration data, (2) a data processing pipeline that analyzes and predicts gas concentration trends using advanced time series models, and (3) a decision-support module that classifies hazard levels and triggers early warnings. At the core of this system is a hybrid analytical approach combining gas concentration prediction and hazard assessment. The prediction module employs optimized time series algorithms to forecast future gas concentrations based on collected data patterns, while the hazard classification module evaluates these predictions against toxicity thresholds using human vulnerability models.

This dual analysis enables dynamic hazard assessment, transitioning from reactive to proactive safety management. The developed software architecture seamlessly integrates these analytical capabilities with wearable hardware, featuring real-time data acquisition (1 Hz sampling frequency), edge-based predictive computation, and multi-mode alert systems. This integration creates a closed-loop workflow from environmental sensing to hazard visualization, providing both individual firefighters and command centers with critical decision-making support during firefighting operations.

2.2. Hazardous gas monitoring and early warning

A hazard prediction process for hazardous gases is constructed with the goal of accurately forecasting hazard levels in firefighting scenarios. The first step involves in-depth analysis of collected gas concentration data. Through this analysis, preliminary parameters for the concentration prediction model are determined, including differencing order, autoregressive order, and moving average order, which form the foundational framework for subsequent predictions and provide critical support for model construction.

The second step focuses on the fitting and optimization of preliminary parameters. By employing a strategy of traversing different parameter combinations derived from the initial parameters, fine-tuning is performed. This process aims to identify the most suitable parameter configuration for predicting leaked gas concentrations, enhancing the model's ability to capture concentration variation patterns and ensuring higher reliability and accuracy in subsequent predictions. Once parameter optimization is complete, the process proceeds to the prediction phase. Using the optimized concentration prediction model, future concentration data can be generated, establishing a connection between current analysis and future hazard trends.

The final step involves hazard level assessment. The predicted gas concentration data, combined with the type of hazardous gas, are matched against predefined hazard level thresholds. Through this matching, the predicted hazard level of the hazardous gas can be accurately evaluated, providing robust quantitative support for safety decision-making and risk mitigation measures. This completes the closed-loop process of hazardous gas monitoring and prediction,



Fig. 1. Firefighting suit system design schematic.

encompassing data analysis, model optimization, and hazard determination, playing a critical role in protecting the safety of individual firefighters. Fig. 2 shows the flowchart of the process of hazardous gas monitoring and early warning.

2.3. Concentration prediction based on time series model

In the prediction of hazardous gas concentrations, the ARIMA model incorporating time series is employed. This method involves several essential steps: initial testing is conducted to determine whether the data exhibit white noise characteristics, as the presence of white noise indicates a lack of predictable structure and precludes further modeling. For data that are not white noise, stationarity testing is performed to ensure the suitability of the series for ARIMA modeling; if the data are non-stationary, appropriate transformations are applied until stationarity is achieved. Following confirmation of stationarity, model identification and parameter estimation are carried out. The resulting model is then subjected to validation procedures, and only validated models are used for forecasting future gas concentration sequences.

Stationarity is a fundamental prerequisite for ARIMA modeling, as non-stationary time series can compromise the validity of statistical inference. In this study, stationarity is assessed using the Augmented Dickey-Fuller (ADF) test, which evaluates the presence of a unit root in the data (Brockwell and Davis, 2016; Said and Dickey, 1984). The null hypothesis of the ADF test posits that the series contains a unit root, indicating non-stationarity. Rejection of the null hypothesis at the 5 % significance level provides statistical evidence that the series is stationary. If the series fails to meet the stationarity criterion, differencing is applied iteratively until stationarity is achieved, with first-order differencing commonly employed to stabilize the mean and variance. Upon confirmation of stationarity, model identification and parameter estimation are conducted to fit the ARIMA model to the transformed data. The fitting formula is as follows:

$$y_t = \mu + \sum_{i=1}^p \phi_i y_{t-i} + \varepsilon_t + \sum_{i=1}^q \theta_i \varepsilon_{t-i} \quad (1)$$

In this formula, y_t represents the value of the time series at time t , μ is the constant term, p and q are the orders of the autoregressive and moving average components respectively, γ_i and θ_i are the model parameters, and ε_t denotes the white noise error term at time t . By applying this formula to the stationary time series data, the ARIMA model parameters are estimated using statistical techniques such as maximum likelihood or least squares; once the optimal parameters are determined, the fitted ARIMA model can be used for forecasting and analysis of future values in the series. The model's performance is evaluated based on the Bayesian Information Criterion (BIC) (Hastie et al., 2009), with the optimal model selected accordingly.

In addition to real-time gas concentration prediction in firefighting environments, the proposed algorithm incorporates the Gauss-Hermite quadrature method to calculate the cumulative exposure dose experienced by firefighters during prolonged operations. This numerical integration technique utilizes Hermite polynomials and the corresponding Gaussian nodes to perform curve fitting on discrete sampling data points. Specifically, it approximates the integral of a one-dimensional real function $f(x)$ over the interval $(-\infty, +\infty)$ as (Press et al., 2007):

$$\int_{-\infty}^{\infty} e^{-x^2} f(x) dx \approx \sum_{i=1}^n W_i f(X_i) \quad (2)$$

In this formula, X_i are the Gaussian nodes (integration points), and W_i are the corresponding weights used in the Gauss-Hermite quadrature. n represents the number of Gaussian nodes (or integration points) used in the Gauss-Hermite quadrature approximation.

2.4. Hazard classification based on human vulnerability models

The proposed firefighting suit design adopts the human vulnerability models to classify the hazard levels based on the hazardous gas concentration (Finney, 1971). The model is designed to estimate individual and societal risk indices, where vulnerability (the probability of fatality for exposed individuals) is calculated based on physical impacts and

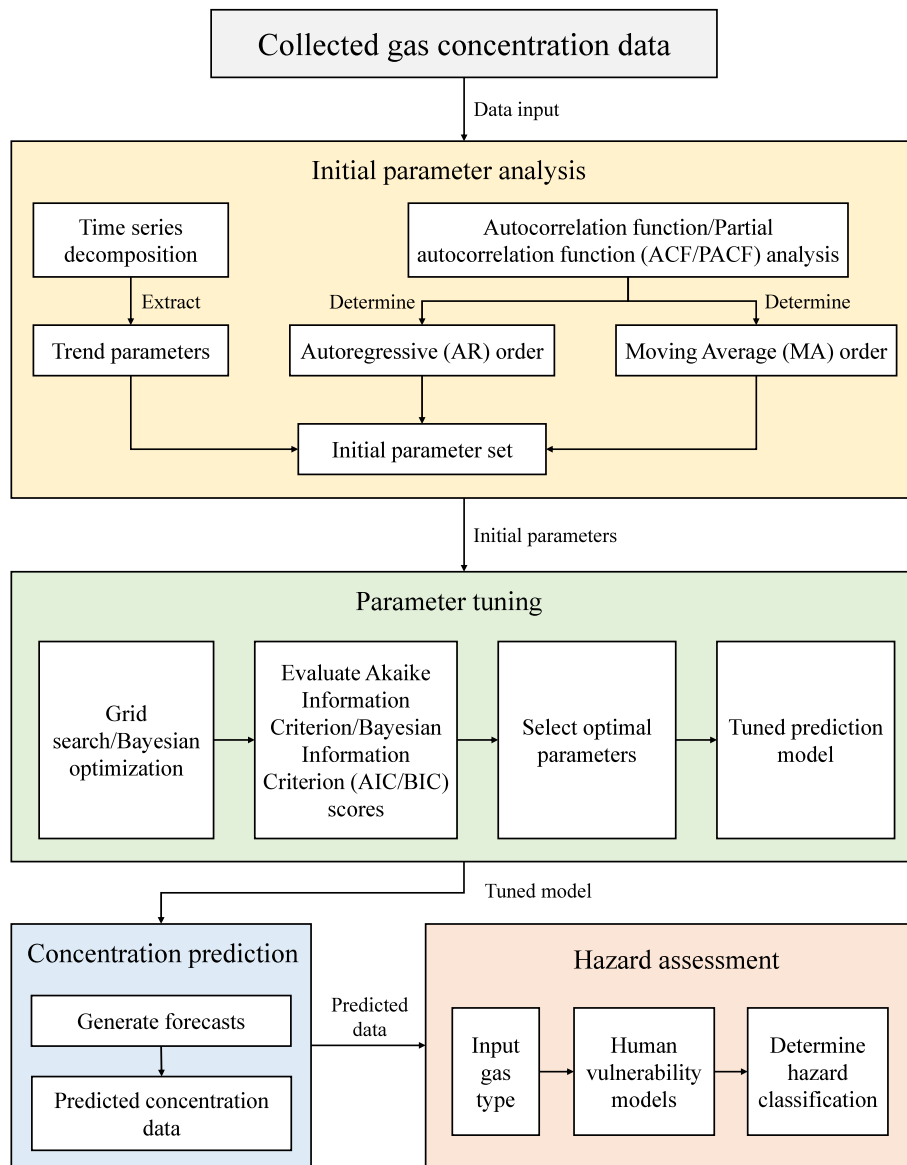


Fig. 2. Flowchart of the process of hazardous gas monitoring and early warning.

estimated exposure duration using a probit model of human vulnerability. The model employs an injury factor Y to represent the harm caused by different gas concentrations to the human body. The formula is as follows (Lees, 2012):

$$Y = a + b \ln(C^n t) \quad (3)$$

where a , b , and n are gas-specific constants representing their respective effects on the human body, C denotes gas concentration (ppm), and t represents the exposure time (min). This model establishes a quantitative relationship that describes the cumulative harm to the human body from prolonged exposure to varying concentrations of toxic gases.

By applying the probit model, the probability of fatality at a given location can be quantitatively derived from the corresponding injury factor for each event. This probabilistic approach enables the assessment of dose-effect relationships for human exposure to hazardous gases, utilizing the cumulative normal (Gaussian) probability distribution function to relate injury factors to vulnerability outcomes. The formula is as follows (National Fire Protection Association, 2018):

$$V = \frac{1}{\sigma\sqrt{2\pi}} \int_{-\infty}^{Y-5} e^{-u^2/2} du \quad (4)$$

Where V represents the lethality probability, and σ denotes the standard normal cumulative distribution function.

The integrated firefighting suit system we've designed and produced can monitor and predict 10 common fire-scene hazardous gases, including toxic gases like CO, HCl, NO₂ and flammable gases CH₄ and H₂. The system also establishes hazard classification criterion for each gas type based on the human vulnerability models.

3. Case study

To systematically evaluate the hazardous gas concentration prediction accuracy, hazard classification precision, and early-warning response effectiveness of the integrated active protective firefighting suit, a comprehensive experimental study was conducted in a training base of city fire brigade in Hebei, China. The experiments simulated fire scenarios by releasing toxic gases and combustible gases, to replicate the actual firefighting environments. Firefighters wore the integrated firefighting suit we designed to verify its ability to monitor, predict, and warn of hazardous gas concentrations. Fig. 3 shows the firefighting suit system modeling of the training base. Fig. 4 shows the firefighters wearing the firefighting suit and the software analyzing gas data.



Fig. 3. 3D model of the training base generated by the firefighting suit software.

3.1. Data collection

The training center consisted of a sealed steel structure (30 m(L) \times 20 m(W) \times 8 m(H)). The experiment involved continuously releasing hazardous gases (CH_2O and CH_4) into the center of the building, and using a firefighting suit system to collect gas concentration data.

The dynamic concentrations of the other eight toxic and flammable gases were simulated based on the collected CH_2O and CH_4 concentration time series to create a multi-gas prediction benchmark with realistic temporal dynamics. Specifically, each simulated gas sequence S_j was created using linear transformations, time lags, and additive Gaussian noise applied to the measured CH_2O and CH_4 data:

$$S_j(t) = \alpha_j C_{\text{CH}_2\text{O}}(t) + \beta_j C_{\text{CH}_4}(t + \delta_j) + N(0, \sigma_j^2) \quad (5)$$

where α_j and β_j are scaling factors, β_j is a small time lag (positive or negative) introduced to create phase differences, and N is Gaussian noise. This approach preserves the general non-stationary trends of the real fire environment while producing diverse, physically plausible concentration profiles for each gas.

Real-time concentration data for 10 representative toxic and hazardous gases were collected during a 270-s monitoring period. The collected hazardous gas concentrations are shown in Table 1.

3.2. Concentration prediction

The ARIMA time series model was employed to predict the concentrations of 10 gases over the next five periods (10–50 s) based on collected data. Table 2 shows the predicted concentrations of the gases. Fig. 5 shows the curves of the collected and predicted concentrations of the 10 gases. The predictions demonstrated a consistent upward trend for most gases, aligning with experimental observations. The results validated the model's capability to capture temporal trends, supporting proactive hazard classification.

3.3. Hazard classification

Applying the collected and predicted gas concentration data, this study implemented a hierarchical classification method to assess hazard levels of toxic and flammable gases based on the human vulnerability models. The classification algorithm is developed through establishing a dose-effect relationship model that correlates gas concentration with exposure duration, while incorporating specific toxicity and flammability characteristics of each hazardous gases, shown as Figs. 6 and 7. Toxic gas hazard classification is based on the probability of death from 1 min of inhalation. The classification thresholds are: low: $<1\%$, $1\% \leq$ moderate $<10\%$, $10\% \leq$ high $<50\%$, and $50\% \leq$ extreme. The hazard classification of flammable gases is based on the ratio of volume concentration to the lower explosion limit (LEL): low: $<10\%$, $10\% \leq$ moderate $<25\%$, $25\% \leq$ high $<50\%$, and $50\% \leq$ extreme. The hazard classification thresholds can be adjusted according to different standards in different application scenarios.

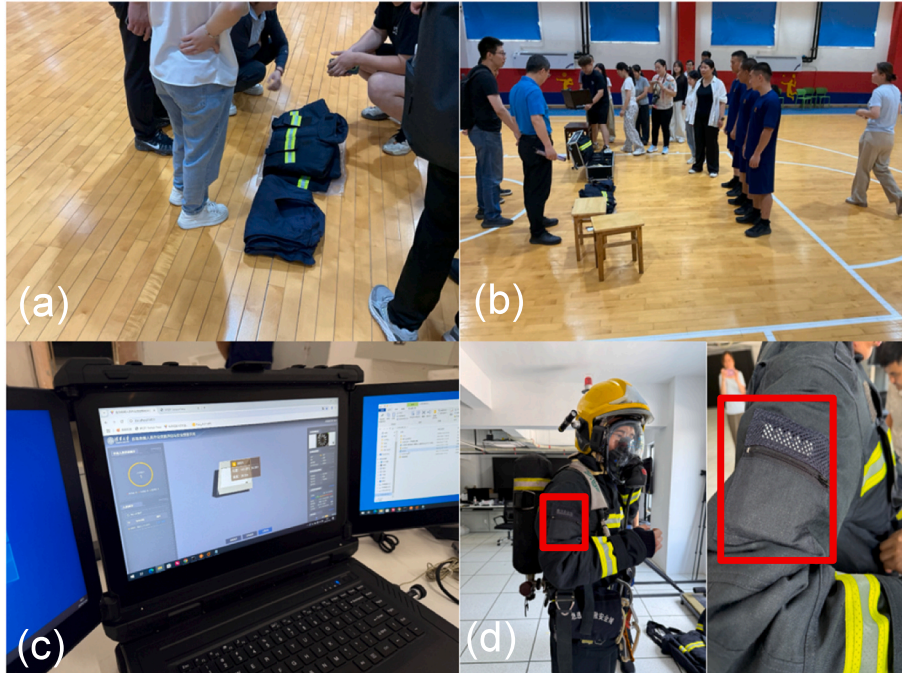


Fig. 4. (a) (b) Firefighters wear the firefighting suits; (c) The software interface analyzing real-time and predicted gas data; (d) Close-up view of the multi-gas sensor module integrated into the suit (red frame).

Table 1

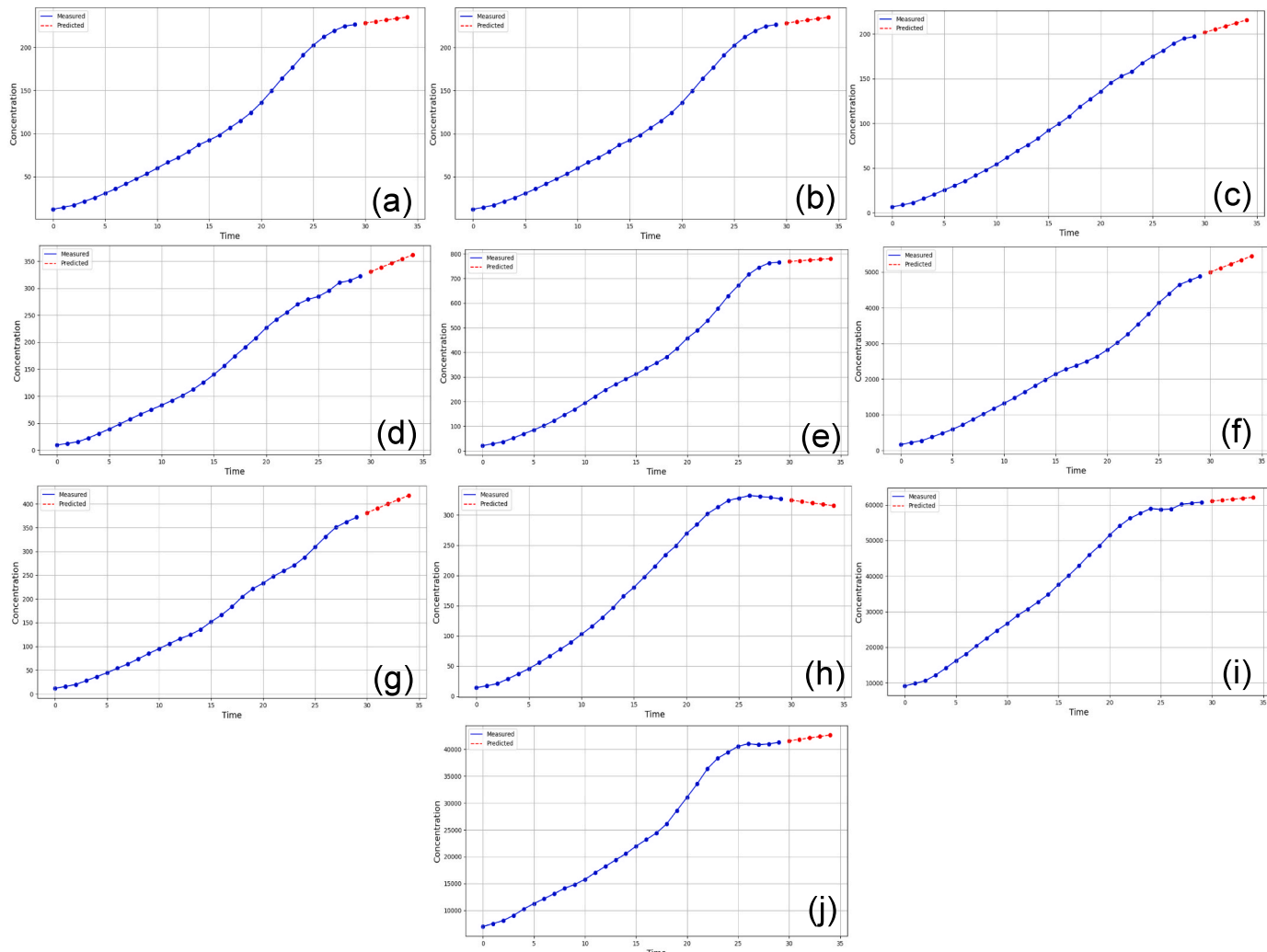
The collected hazardous gas concentration data (partial data).

Time period (10s)	Gas concentration (ppm)									
	HCl	HCN	NO ₂	SO ₂	HF	CO	CH ₂ O	H ₂ S	H ₂	CH ₄
3	46.46	16.95	11.24	15.52	36.47	270.02	19.80	20.78	10,598.39	8149.59
6	112.28	30.76	25.48	39.13	84.96	589.28	44.49	45.55	16,255.97	11,300.56
9	197.73	47.62	41.67	66.72	146.42	1021.55	73.58	77.69	22,554.59	14,130.62
12	301.45	66.59	61.51	92.01	220.94	1469.56	105.66	115.43	28,929.75	17,050.25
15	398.93	86.88	83.11	125.53	291.54	1983.33	135.83	165.35	34,822.16	20,557.08
18	507.35	106.82	107.74	174.31	357.13	2376.88	183.28	214.82	42,884.91	24,422.47
21	609.99	136.09	135.54	226.61	457.61	2818.41	232.96	269.28	51,549.69	31,058.66
24	692.54	176.89	157.62	270.23	577.26	3543.90	270.95	312.99	57,656.07	38,314.10
27	793.96	212.17	181.40	295.26	716.32	4391.76	330.83	332.17	58,823.27	41,012.02

Table 2

The predicted hazardous gas concentration data.

Time period (10s)	Gas concentration (ppm)									
	HCl	HCN	NO ₂	SO ₂	HF	CO	CH ₂ O	H ₂ S	H ₂	CH ₄
30	883.32	228.32	201.57	330.59	769.13	5001.61	381.41	324.34	61,084	41,544.56
31	899.03	230.1	205.09	338.48	772.08	5116.25	390.77	322.03	61,359.49	41,822.55
32	914.56	231.85	208.59	346.3	774.93	5229.28	399.95	319.76	61,620.46	42,097.76
33	929.93	233.56	212.06	354.06	777.71	5340.73	408.96	317.52	61,867.68	42,370.22
34	945.13	235.24	215.5	361.74	780.41	5450.6	417.8	315.33	62,101.88	42,639.96

**Fig. 5.** The collected and predicted concentration trends for the 10 hazardous gases (blue: collected data, red: predicted data, ppm). (a) HCl (b) HCN (c) NO₂ (d) SO₂ (e) HF (f) CO (g) CH₂O (h) H₂S (i) H₂ (j) CH₄.

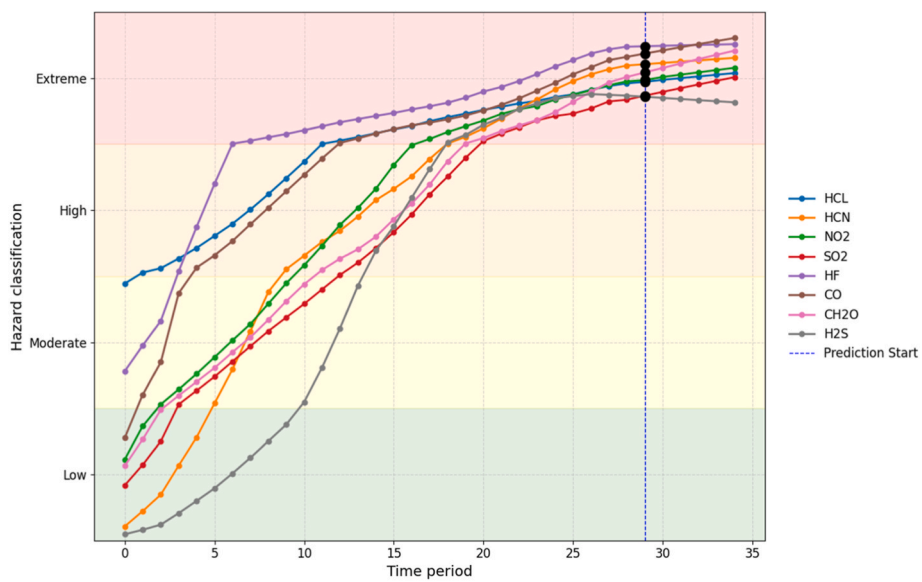


Fig. 6. The hazard classification of toxic gases based on collected and predicted data.

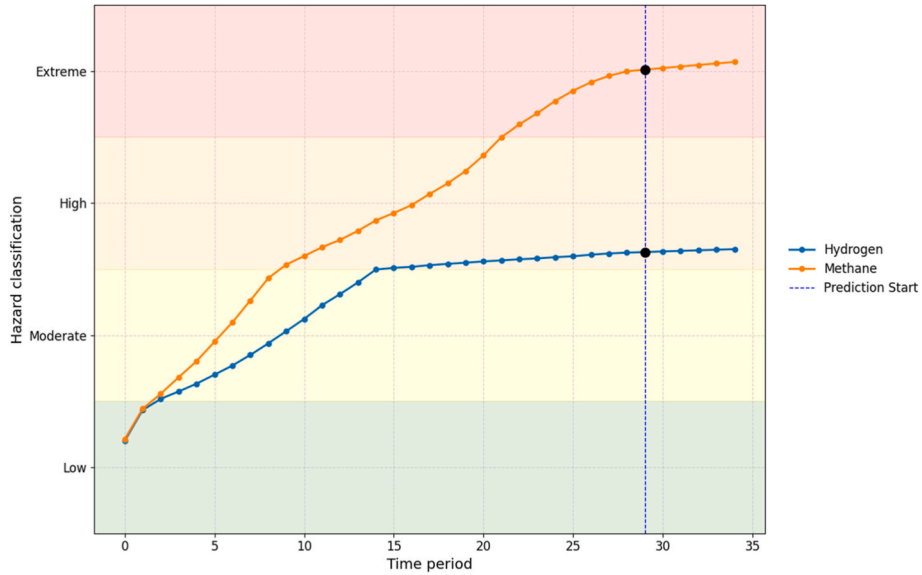


Fig. 7. The hazard classification of flammable gases based on collected and predicted data.

By implementing gas-specific classification thresholds, the system achieved real-time dynamic monitoring and evaluation of multiple hazardous gases. This integrated system provides accurate and timely risk warnings for firefighters during operational scenarios, significantly enhancing situational awareness and personnel safety.

3.4. Quality analysis of predicted results

Quantitative analysis was performed using Root Mean Square Error (RMSE), Mean Absolute Error (MAE), and Mean Absolute Percentage Error (MAPE), with results in Table 3. RMSE reflects the overall

Table 3
The quality analysis of predicted results.

Gas	MAE	MAE equality	RMSE	RMSE equality	MAPE (%)	MAPE equality	data range
HCl	849.397	normal	988.3334	normal	3.3204	excellent	2840.625
HCN	699.378	normal	863.9093	normal	8.7166	excellent	3217.886
NO ₂	1187.832	good	1416.921	poor	20.1496	normal	3256.145
SO ₂	729.9107	poor	827.1249	poor	8.2941	excellent	1685.239
HF	994.73	good	1137.727	good	5.0695	excellent	5033.214
CO	10,518.52	normal	12,777.64	normal	9.2604	excellent	36,693.05
CH ₂ O	529.5385	good	589.8763	good	5.2447	excellent	2968.54
H ₂ S	343.9053	good	395.637	excellent	3.4175	excellent	2737.886
H ₂	76,963.79	good	100,783.9	good	3.9074	excellent	486,603.2
CH ₄	75,981.6	poor	83,685.18	poor	7.271	excellent	223,219.8

magnitude of prediction errors and is sensitive to large deviations; MAE represents the average absolute error, offering an intuitive measure of typical prediction accuracy; and MAPE expresses the average error as a percentage of actual values, facilitating comparison across different datasets or scales.

The results demonstrate significant variations in the model's predictive performance across different gases. For instance, H₂S exhibited "excellent" performance in both RMSE and MAPE metrics, with an MAE of 343.9053 and an exceptionally low MAPE of 3.4175 %, indicating high prediction accuracy. Similarly, CH₂O showed "good" performance in both MAE and RMSE, while achieving an "excellent" MAPE of 5.2447 %, suggesting reliable prediction outcomes.

However, the model demonstrated poorer performance for certain gases, such as SO₂ and CH₄, which received "poor" ratings for both MAE and RMSE, despite maintaining "excellent" MAPE scores (8.2941 % and 7.271 %, respectively). This discrepancy may stem from the substantially larger data ranges of these gases (SO₂: 1685.239; CH₄: 223219.8), resulting in higher absolute errors while maintaining relatively low percentage errors. Notably, H₂ and CO exhibited high absolute errors (e.g., H₂'s MAE reached 76,963.79), yet achieved "excellent" MAPE performance (3.9074 % and 9.2604 %, respectively), underscoring the necessity of considering both absolute and relative error metrics when evaluating model performance.

Based on historical gas concentration data from time periods 0–24, time series models were employed to predict gas concentrations at time periods 25–29. Subsequently, actual experimental measurements were simultaneously collected at these time points to serve as validation benchmarks. By conducting point-by-point comparisons between predicted and measured values, the model's prediction accuracy and early warning capability were evaluated, as shown in **Table 4**.

The analysis of the results indicates that the gas concentration prediction model achieves an average accuracy of 96.25 %, demonstrating strong predictive capability for future data. Among the tested gases, SO₂, NO₂, and HCl exhibit the highest precision (accuracy >99 %), whereas H₂ and CH₄ show relatively larger errors while still maintaining an overall accuracy above 90 %. Further optimization of the model is recommended to improve prediction performance for gases with higher errors.

In summary, the model demonstrates superior predictive capability for gases with smaller data ranges (e.g., H₂S, CH₂O), while showing limitations for gases with larger ranges or higher volatility (e.g., CH₄, SO₂). Although most gases achieved "excellent" MAPE levels, indicating effective control of relative errors, further optimization is required—particularly in reducing absolute errors for gases like CH₄ and SO₂—to enhance overall prediction accuracy.

4. Advantages of the application of time series modeling

Previous hazard classification methods for firefighting scenarios rely on comparing real-time monitored gas concentration data to preset thresholds, constituting a "passive response" assessment. The fundamental limitation of these traditional methods, such as threshold-based

Table 4
The accuracy of the prediction algorithm.

Gas	Average Error	Average Accuracy
HCl	7.51	99.09
HCN	15.37	93.10
NO ₂	1.94	99.00
SO ₂	2.35	99.21
HF	51.55	93.17
CO	109.84	97.70
CH ₂ O	9.63	97.21
H ₂ S	28.03	91.47
H ₂	4660.89	92.24
CH ₄	1510.89	96.32

alarms and moving average techniques, is their inherent lack of predictive capability. This often leads to delayed warnings or misjudgments when gas concentrations change rapidly. In contrast, our proposed ARIMA model directly addresses this gap by providing proactive forecasting. We quantify its superiority by highlighting the achieved 50-s early-warning time and 96.25 % prediction accuracy—benefits that are unattainable by passive threshold systems. Furthermore, compared to simpler techniques like moving averages, the ARIMA model's ability to capture complex temporal trends and nonlinear dynamics is evidenced by its high accuracy across multiple gases, enabling it to anticipate sudden concentration spikes that would overwhelm conventional methods. For example, in the 2015 Tianjin Port explosion accident, concentrations of toxic gases (e.g., HCN) rose sharply in a short time. Traditional classification methods, lacking predictive capabilities, failed to guide firefighters to evacuate in advance, ultimately resulting in casualties.

The time series analysis introduced in this study can generate rolling predicted concentration curves for the next 5–10 min by mining time series characteristics of collected concentration data, upgrading hazard classification from "real-time judgment" to "trend prediction." Compared with previous monitoring and warn methods that do not use time series algorithms, in simulated experiments for H₂S leakage scenarios, traditional methods only alarmed when the concentration reached 30 ppm (moderate risk). In the analysis of prediction accuracy and early warning timeliness, the time-series model demonstrated the capability to predict post-event thresholds within the next 50 s with an accuracy of 91.47 %, thereby providing firefighters with critical reaction time to adjust their routes.

For the common sudden concentration spikes in fire scenes (a sharp increase in gas concentration caused by deflagration), the time series model can capture subtle early concentration fluctuation signals, adjusting the hazard level in advance (e.g., directly predicting from "low risk" to "high risk"). In contrast, traditional methods must wait for stable concentrations before classification, easily missing the optimal response opportunity.

5. Conclusion

Firefighters face life-threatening exposure to toxic and flammable gases during firefighting operations. Traditional firefighting suits remain limited by passive protection mechanisms, lacking real-time gas concentration prediction and dynamic early-warning capabilities. Existing research predominantly focused on improving physical properties of suits, neglecting the integration of active monitoring and intelligent prediction for dynamic fire environments.

This study develops an advanced active-protection firefighting suit system that integrates real-time gas monitoring, predictive analytics, and early warning functions. By combining a hybrid ARIMA prediction model with a human vulnerability probit model, the system achieves accurate gas concentration forecasting and dynamic risk assessment. The hardware-software co-designed prototype demonstrates strong performance in simulated environments, providing 50 s early warnings with 91.47–99.21 % prediction accuracy depending on gas characteristics.

The research highlights the potential of intelligent protective equipment through its three key innovations: (1) The firefighting suit system integrates an ARIMA time series model with human vulnerability probit models to predict toxic gas concentrations and assess hazards in fire scenarios; (2) Leveraging predicted data and vulnerability models, the system can dynamically adjust hazard classifications to provide actionable evacuation or tactical guidance. (3) The system embeds multi-gas sensors, edge computing modules, and a visualization interface to establish a closed-loop workflow from data acquisition to decision-making support.

Despite the promising results, this study has several limitations that warrant attention in future research. First, the environmental robustness

of the system, including its performance under extreme conditions such as very high temperatures, dense smoke, and water exposure, requires further validation through large-scale field tests. Second, the generalizability of the prediction model needs enhancement to handle highly unpredictable events, such as sudden explosions that cause instantaneous and non-linear changes in gas concentrations. Integrating additional sensors (e.g., for pressure and optical density) and exploring more complex AI models could address this. Third, the long-term durability and reliability of the integrated wearable sensors and computing modules in harsh firefighting conditions need to be thoroughly evaluated and improved. Future work will focus on addressing these limitations to advance the practical deployment of intelligent firefighting equipment.

This study establishes a foundation for the design of intelligent firefighting suits, demonstrating how the integration of predictive algorithms with protective gear can significantly improve firefighter safety and operational effectiveness in hazardous environments. The research results are expected to be applied in actual fire brigades, to reduce casualties among firefighters in fire scenes.

CRediT authorship contribution statement

Yiwei Peng: Writing – original draft, Methodology. **Wenguo Wang:** Supervision, Project administration. **Xinyan Huang:** Writing – review & editing, Supervision. **Zhichao He:** Writing – review & editing, Writing – original draft, Supervision, Funding acquisition.

Declaration of competing interest

The authors declare that they have no known competing financial interests or personal relationships that could have appeared to influence the work reported in this paper.

Acknowledgement

This study was supported by the National Key Research and Development Program of China (Grant No. 2023YFC3008700), the National Natural Science Foundation of China (Grant Nos. 72404160, 72442008, 72521001, 72034004), and the Hong Kong Research Grants Council Theme-based Research Scheme (T22- 505/19-N).

Data availability

Data will be made available on request.

References

Blecha, T., Soukup, R., Kaspar, P., Hamacek, A., Reboun, J., 2018. Smart firefighter protective suit-functional blocks and technologies. In: 2018 IEEE International Conference on Semiconductor Electronics. Kuala Lumpur, Malaysia, p. C4. <https://doi.org/10.1109/smelec.2018.8481335>.

Brockwell, P.J., Davis, R.A., 2016. *Introduction to Time Series and Forecasting*, third ed. Springer, New York, NY, USA, pp. 120–150.

Chen, Y., Su, Y., Li, G., Zhao, P., Tian, M., Li, J., 2024. Design and performance evaluation of a firefighting protective suit with an incorporated liquid-cooled system. *Int. J. Occup. Saf. Ergon.* 30 (1), 205–214. <https://doi.org/10.1080/10803548.2023.2235144>.

Cheng, Z., Ren, G., Dong, S., Li, R., Huo, Z., Li, J., 2023. Effective navigation for an emergency response for firefighters with wearable haptic displays design. In: 2023 IEEE 6th International Conference on Knowledge Innovation and Invention (ICKII), pp. 46–49. <https://doi.org/10.1109/ickii58656.2023.10332748>.

China Chemical Safety Association, 2016. Tianjin port special major fire and explosion accident investigation report published. Available: <http://www.chemicalsafety.org.cn/index.php/article/omwvzno04qn1kdyq>. (Accessed 10 August 2025).

China National Emergency Broadcasting (CNEB), 2019. Chemical leak in Melbourne, Australia sends 7 people to hospital. Available. <http://www.cneb.gov.cn/2019/05/09/ART11557393804556648.shtml>. (Accessed 10 August 2025).

Couto, L., Avelar, M., Bernardes, V., Rocha, L., 2023. Inhalation of toxic gases in the kiss nightclub disaster: an example of inhalation injury from indoor fires. *Collect. Int. Top. Health Sci.* 1, 18–30. <https://doi.org/10.56238/colleinternalthescienv1-003>.

Dong, X., Ma, Y., Zhang, S., Rong, C., Jiang, X., Li, Y., Nie, S., Tian, K., 2025. Rigorous fireproofing, thermal protection, graded fire alarm and body language recognition: designing nano-coated aramid for smart firefighting clothing. *Adv. Fiber Mater.* 7, 1545–1562. <https://doi.org/10.1007/s42765-025-00569-y>.

European Committee for Standardization, 2020. Protective Clothing for Firefighters - Performance Requirements for Protective Clothing for Firefighting. CEN, Brussels, Belgium. <https://doi.org/10.3403/30235983>. Rep. EN 469:2020.

Finney, D.J., 1971. *Probit Analysis*. Cambridge University Press, Cambridge, UK. <https://doi.org/10.1002/bimj.19720140111>.

Hastie, T., Tibshirani, R., Friedman, J., 2009. *The Elements of Statistical Learning*, second ed. Springer, New York, NY, USA, pp. 219–259. <https://doi.org/10.1007/bf02295616>.

Hur, P., Rosengren, K.S., Horn, G.P., Smith, D.L., 2013. Effect of protective clothing and fatigue on functional balance of firefighters. *J. Electromyogr. Kinesiol.* 23 (2), 478–484. <https://doi.org/10.4172/2165-7556.s2-004>.

Lees, F.P., 2012. *Lees' Loss Prevention in the Process Industries*, fourth ed. Butterworth-Heinemann, Oxford, UK. <https://doi.org/10.1016/c2009-0-24104-3>.

Mandal, S., Camenzind, M., Annaheim, S., Rossi, R.M., 2018. Firefighters' protective clothing and equipment. In: *Firefighters' Clothing and Equipment*. CRC Press, Boca Raton, FL, pp. 31–59. <https://doi.org/10.1201/978042944876-2>.

Ministry of Public Security of China, 2014. Firefighters' protective clothing for fire fighting. MPS, beijing, China. Rep GA, 10–2014. <https://doi.org/10.3403/03029031u>.

National Fire Protection Association, 2018. *Standard on Protective Ensembles for Structural Fire Fighting and Proximity Fire Fighting*. NFPA, Quincy, MA, Rep. NFPA 1971.

Press, W.H., Teukolsky, S.A., Vetterling, W.T., Flannery, B.P., 2007. *Numerical Recipes: the Art of Scientific Computing*, third ed. Cambridge University Press, Cambridge, UK, pp. 161–175.

Said, S., Dickey, D.A., 1984. Testing for unit roots in autoregressive-moving average models of unknown order. *Biometrika* 71 (3), 599–607. <https://doi.org/10.2307/2336570>.

Shakeriaski, F., Ghodrat, M., Rashidi, M., Samali, B., 2022. Smart coating in protective clothing for firefighters: an overview and recent improvements. *J. Ind. Text.* 51 (5 Suppl. I), 7428S–7454S. <https://doi.org/10.1177/15280837221101213>.

Spitzenberger, C., Johnson, C., Le, M., Mshelia, A., Pitblado, R., 2016. *Strike the Right Balance between Active and Passive Fire Protection*. American Institute of Chemical Engineers, CEP, pp. 61–68.

U.S. Occupational Safety and Health Administration, 2013. Available: Yarnell Hill Fire, Wildfires. <https://www.osha.gov/disaster/wildfires/yarnell-hill-fire>. (Accessed 10 August 2025).

Xu, D., Chen, Z., Liu, Y., Ge, C., Gao, C., Jiao, L., Guo, W., Zhang, Q., Fang, J., Xu, W., 2023. Hump-Inspired Hierarchical Fabric for Personal Thermal Protection and Thermal Comfort Management. *Adv. Funct. Mater.* 33 (10), 2212626. <https://doi.org/10.1002/adfm.202212626>.

Xu, H., Zhang, L., Jin, Z., Cao, B., Wang, A., Liu, Z., 2025. Physiological and perceptual responses of firefighters wearing protective clothing under various training environment and activity conditions. *Build. Environ.* 267, 112247. <https://doi.org/10.1016/j.buildenv.2024.112247>.

Zhang, Y., Huang, X., 2024. Smart safety design for firefighting, evacuation, and rescue. In: *Intelligent Building Fire Safety and Smart Firefighting*. Springer, Cham, Switzerland, pp. 237–255. <https://doi.org/10.1007/978-3-031-48161-110>.

Zhang, Y., Zhang, X., Huang, X., 2023. Design a safe firefighting time (SFT) for major fire disaster emergency response. *Int. J. Disaster Risk Reduct.* 88, 103606. <https://doi.org/10.1016/j.ijdr.2023.103606>.